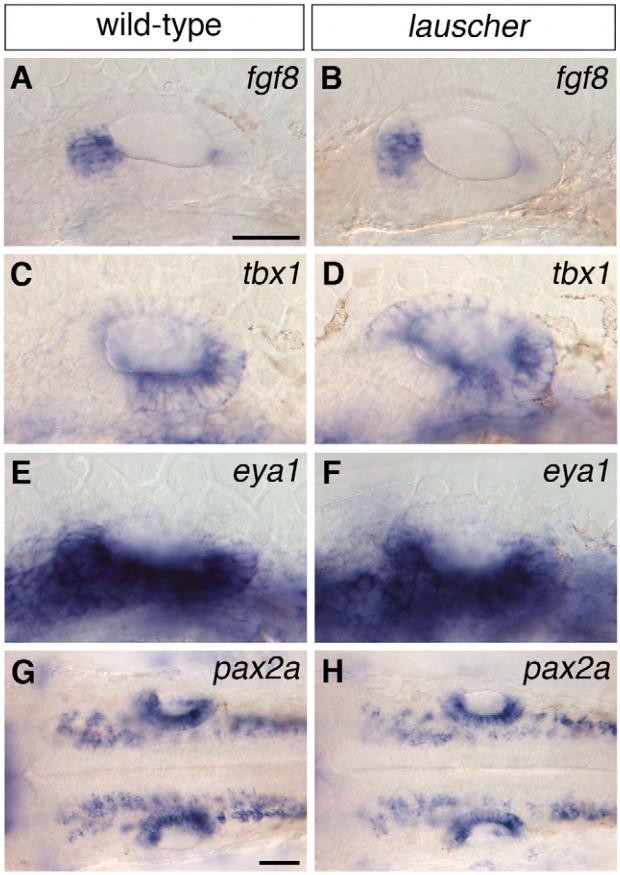

Figure S1. Expression of early otic patterning markers is normal in *lauscher* mutants. (A-J) Expression of early patterning markers in the otic vesicle is indistinguishable between wild-types and homozygous *lau*^{tb233c} mutants. Normal expression is seen for *fgf8a* (*fgf8*) anteriorly (A,B), *tbx1* posteriorly (C,D), *eya1* ventrally (E,F) and *pax2a* medially (G,H) at 27 hpf. Scale bars: A, 50µm (applies to B-F); G, 50µm (applies to H).

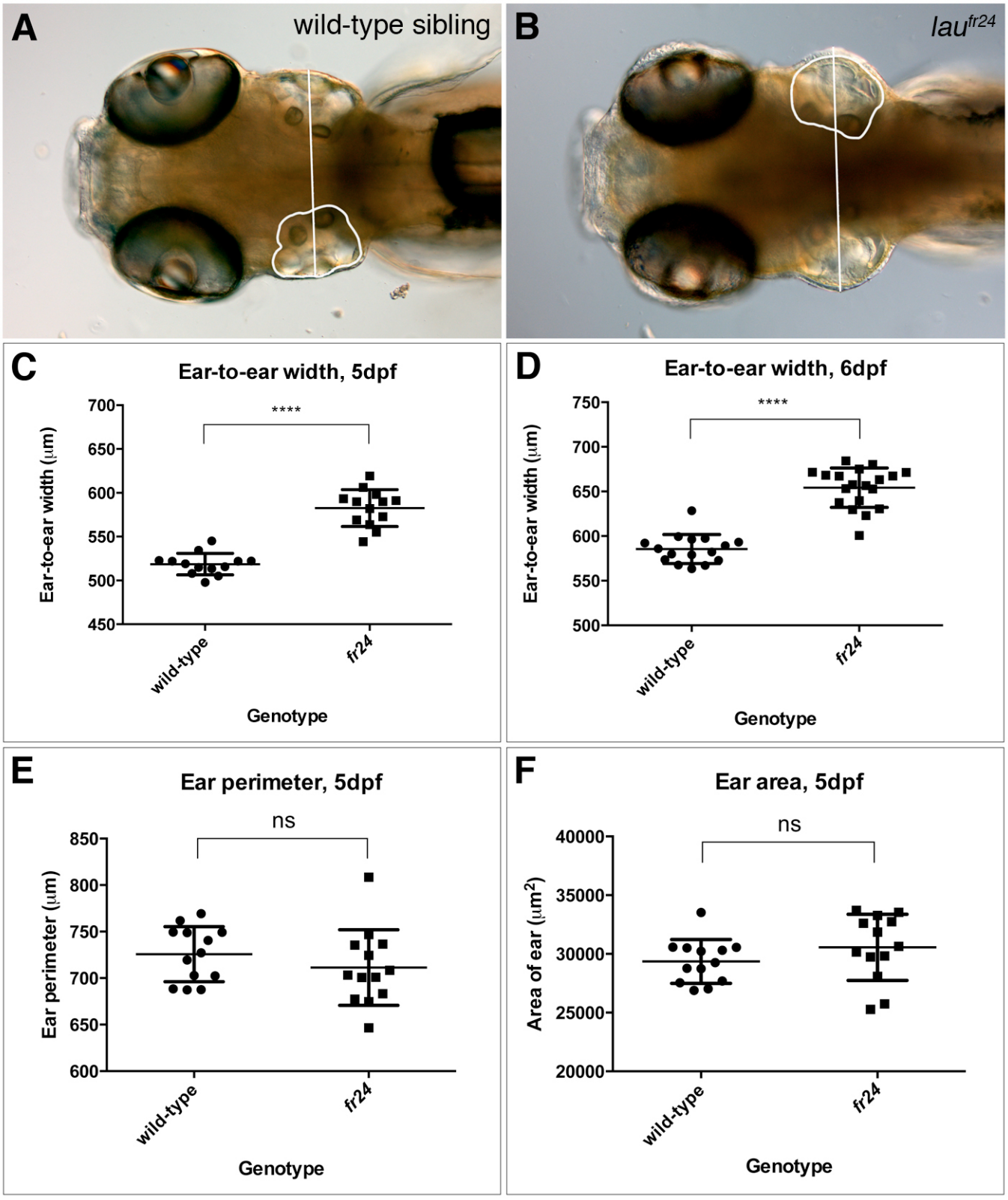

Figure S2. Quantitation of the *lauscher* swollen ear phenotype. (A,B) Sample micrographs showing dorsal views of live wild-type sibling (A) and *lau*^{fr24} mutant (B) embryos at 5 dpf. Measurements were taken of ear-to-ear width (straight white line) and ear perimeter (white line outlining ear) using CELLB software (Olympus). Embryos were treated with 1-phenyl 2-thiourea (PTU) to suppress development of pigmentation. Embryos were photographed at a focal plane that highlighted the largest visible dimensions for the parameters shown, and the ear chosen for measurement in each micrograph was the one with the most clearly visible outline. Ear cross-sectional area was calculated from the perimeter drawn, using CELLB software (Olympus). **(C-F)** Quantitation of ear-to-ear width (C,D), ear perimeter (E) and ear area (F); data were plotted using Prism 6 (GraphPad software). $N \geq 13$ for each data set. Error bars indicate standard deviation; ****$P<0.0001$ (unpaired, two-tailed *t*-test); ns, not significant.

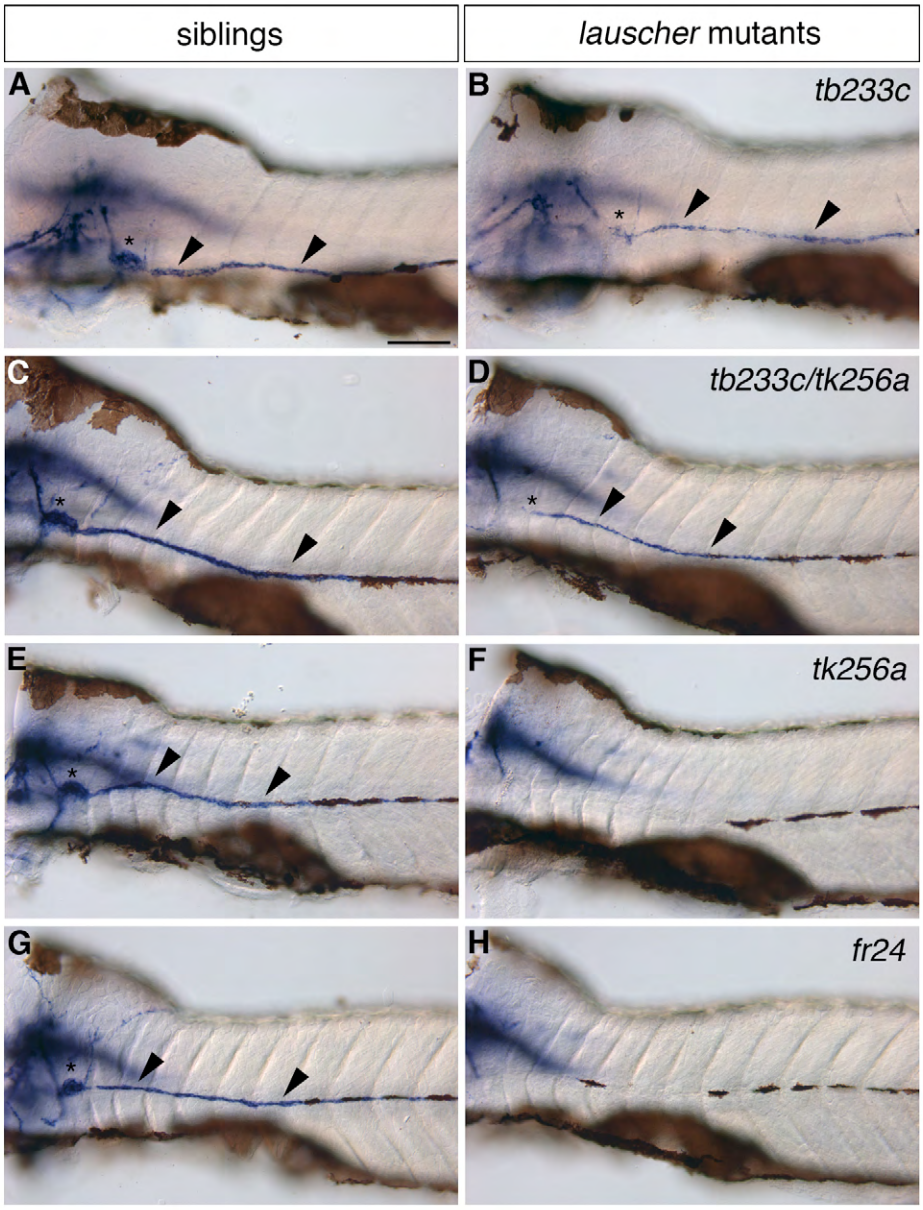

Figure S3. Expression of the *myelin basic protein* gene (*mbpa*) is lost or reduced in the posterior lateral line ganglion and nerve in *lauscher* mutants. (A-H) Whole mount in situ hybridisation at 5 days post fertilisation shows a reduction in *mbpa* (*mbp*) expression in Schwann cells of the posterior lateral line ganglion (asterisks) and nerve (arrowheads) in the hypomorphic *tb233c* homozygotes (B) and *tb233c/tk256a* transheterozygotes (D); expression is lost in *tk256a* (F) and *fr24* homozygotes (H). Lateral views. Scale bar: 100µm throughout.

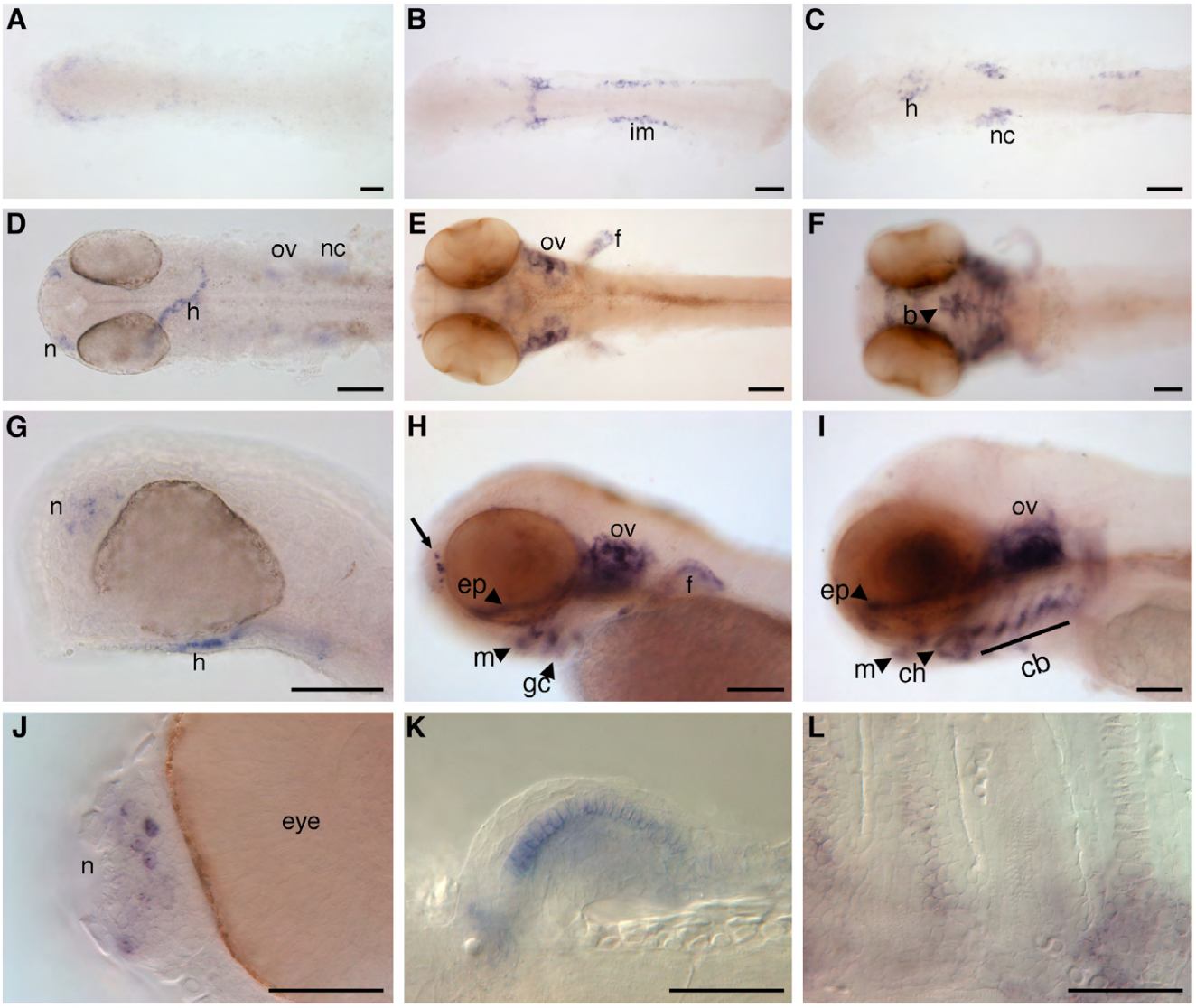

Figure S4. Expression of *gpr126* mRNA at other sites during zebrafish development. (A-C) Flat mounted embryos at 5 somites (A), 14 somites (B) and 23 somites (C). Patchy expression of *gpr126* is seen the anterior of the embryo and also in presumed neural crest (A). At 14 somites, weak expression is seen in the presumed developing heart fields, neural crest and intermediate mesoderm (im; precursor of the pronephric ducts) (B). At 23 somites, expression increases in the migrating heart tube (h) and neural crest (nc) (C). **(D,G,J)** Expression at 24 hpf in dorsal (D), lateral (G) and detailed (J) view, showing expression in the post-otic neural crest (nc), heart tube (h) and olfactory epithelium (nose, n). J shows staining of individual cells within the olfactory epithelium. **(E,H,K)** 48 hpf embryos in dorsal (E), lateral (H) and detailed (K) view. Expression continues in the nose (arrow, H), but is reduced in the heart and lost in the post-otic ganglia. New expression is seen in the ear (ov), pectoral fin (f) and tail fin (not shown), and chondrocytes of the head (arrowheads). K shows expression of *gpr126* in the chondrocytes of the pectoral fin. **(F,I,L)** 72 hpf embryos in dorsal (F), lateral (I) and detailed (L) view. Expression continues in the ear, nose, fins and head chondrocytes (arrowheads and line). Detailed view of *gpr12* expression in posterior ceratobranchials is shown in L. By 96 hpf, expression of *gpr126* remains primarily in the ear (not shown). Abbreviations: b, basihyal; cb, ceratobranchials; ep, ethmoid plate; ch, ceratohyal; f, pectoral fin; gc, gill cartilages; h, heart; im, intermediate mesoderm; m, Meckel's cartilage, n, nose (olfactory epithelium); nc, neural crest; ov, otic vesicle. Scale bars: A-I, 100 µm; J-L, 50 µm.

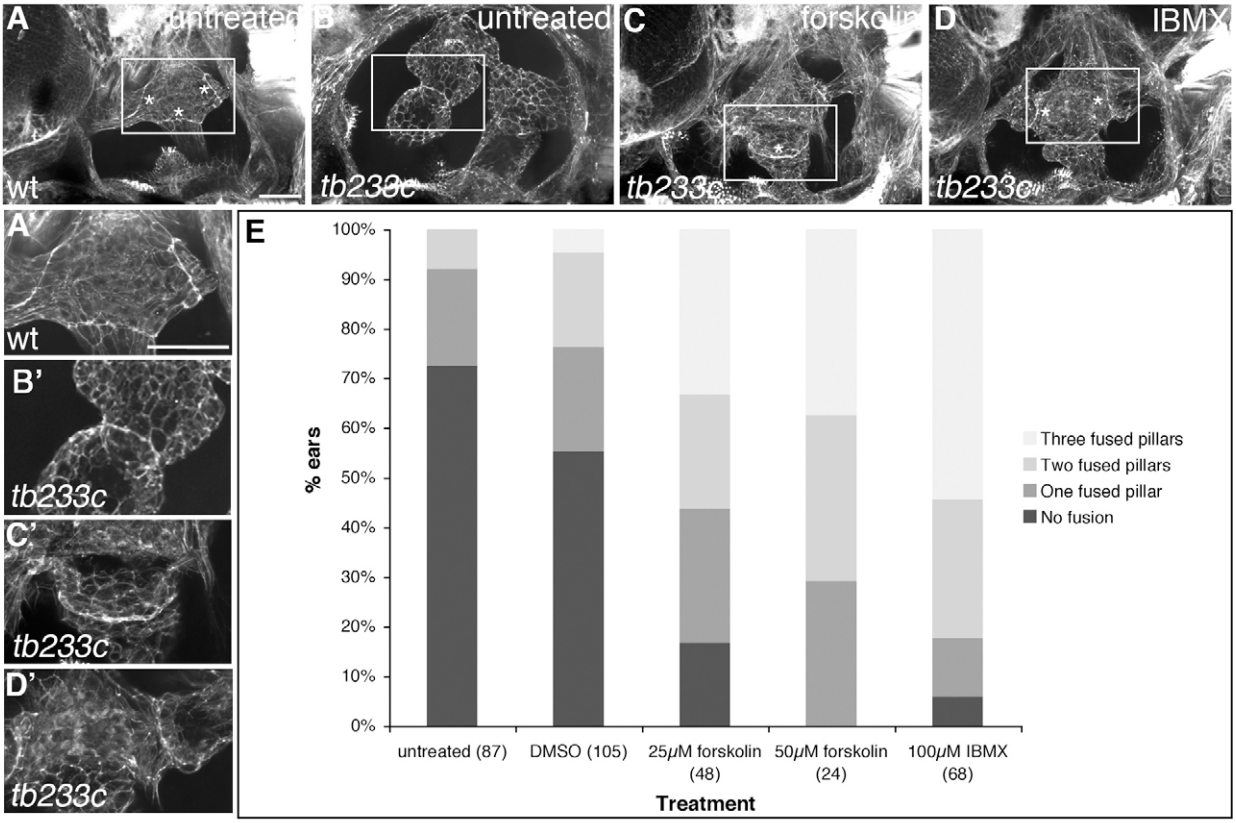

Figure S5. Treatment with cAMP agonists can rescue fusion plate formation in *lauscher* mutant embryos. (A-D') Confocal images of ears stained with FITC-phalloidin (marking F actin) to show morphology of the canal projections and pillars. Concentrations of actin mark the fusion plates (shown at higher magnification in A'-D'). (A, A') Wild-type ear. Three fusion plates are clearly visible (asterisks). (B,B') Untreated ear from a homozygous *tb233c* mutant. Canal tissue is very disorganised. Although projections are touching in this ear, analysis of the z-stack indicated that this was not a true fusion plate. (C-D') Treatment of homozygous *tb233c* embryos with either 50μM forskolin or 100μM IBMX can restore pillar formation. Fusion plates appear relatively normal. **(E)** Quantitation of the number of fusion plates present. Data were analysed with a 4×3 chi-square contingency table (DMSO, forskolin) or a 4×2 chi-square contingency table (DMSO, IBMX); $P<0.001$ for both drugs. *N* numbers are shown in parentheses. Lateral views. Scale bars: A-D 50μm; A'-D' 50μm.

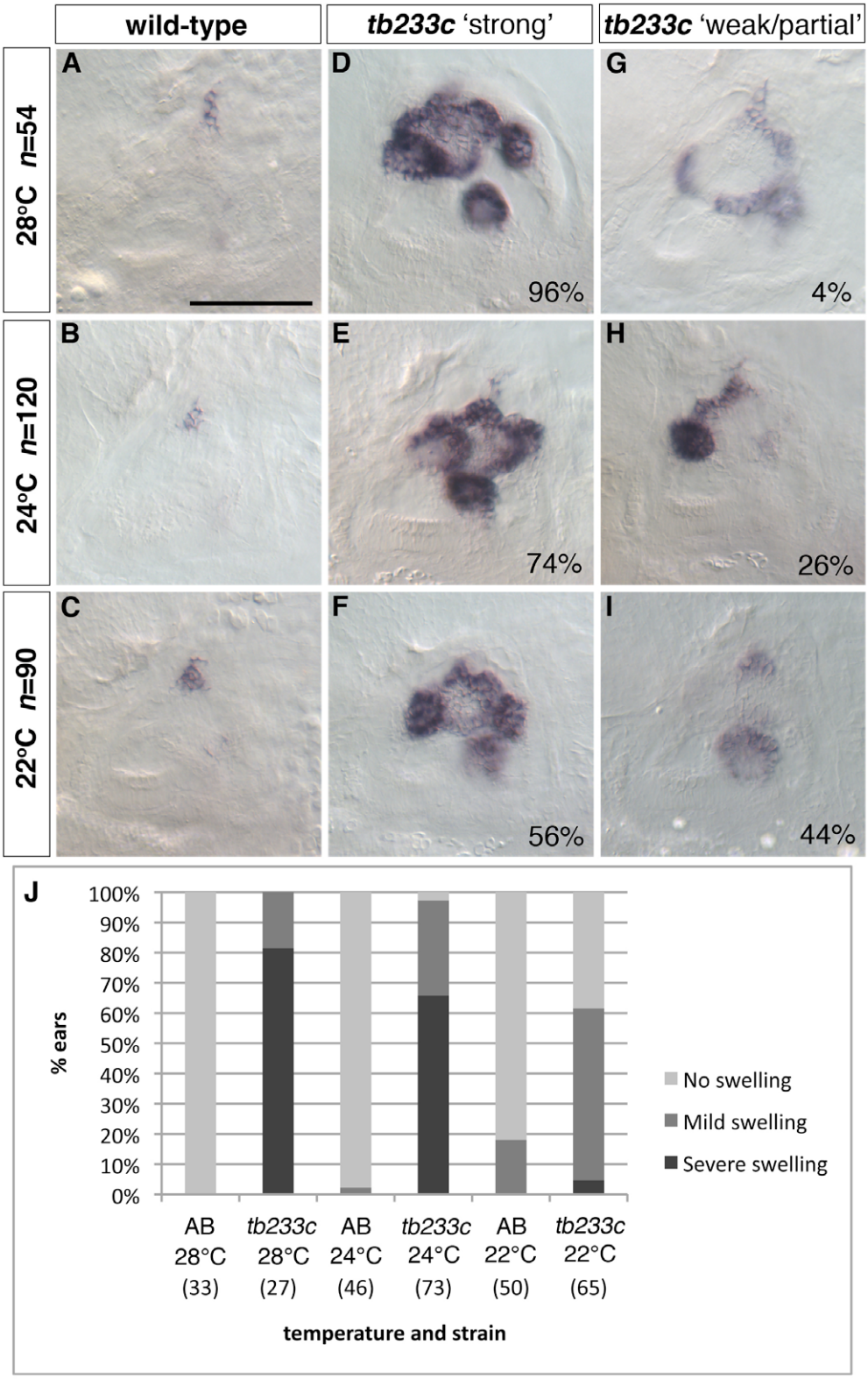

Figure S6. Incubation of *lau*^{tb233c} mutants at a lower temperature throughout the fusion period has a rescuing effect on otic *versican* expression and projection fusion. (**A-I**) Expression of *vcanb* in 4dpf wild-type (A-C), and *tb233c* (B-I) embryos, incubated at 28˚C (A,D,G), 24˚C (B,E,H) and 22˚C (C,F,I). Embryos were initially grown for 24 hours at 28˚C. In wild-type embryos, *vcanb* expression is down-regulated in the fused pillars; staining only remains in the dorsolateral septum (DLS) (A-C). Mutant embryos retain strong *vcanb* expression in the unfused projections (D-F). Some mutant embryos show weaker expression (G) or partial expression where there are fused and unfused pillars in the same ear (H,I). The proportion of embryos showing decreased *vcanb* expression and rescue of fusion increases with a decrease in temperature. Percentages for each phenotypic class are shown on the panels; *N* numbers (number of mutant ears analysed) are shown in the boxes at the left. (**J**) Graphical representation of ear swelling data for wild-type and mutant embryos grown at different temperatures. The rescue of fusion in one or more pillars results in a decrease of swelling in the ear. Embryos grown at lower temperatures have reduced swelling in the ear. *N* numbers (number of mutant ears analysed) are shown in parentheses.

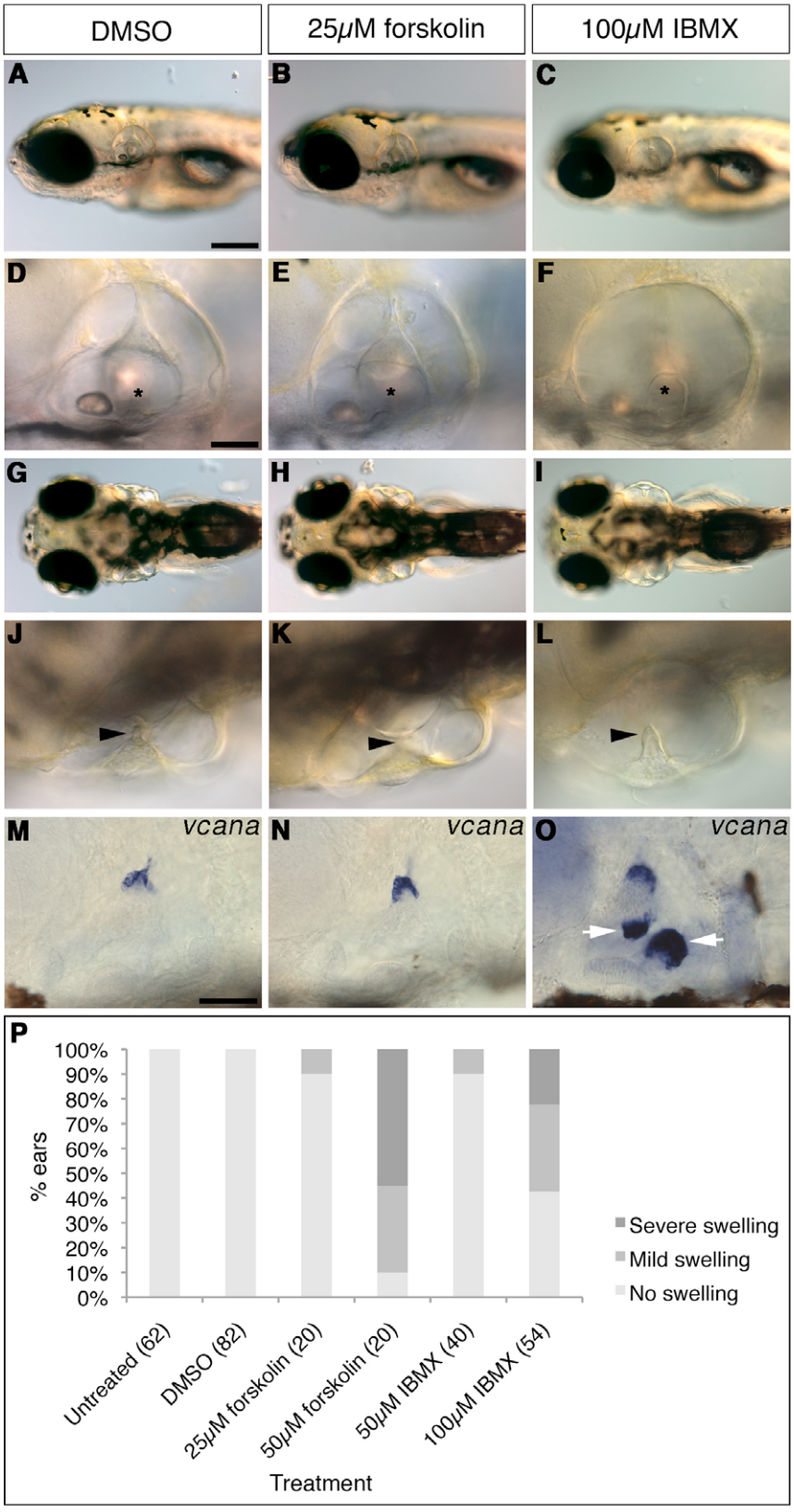

Figure S7. Treatment of wild-type embryos with cAMP agonists results in semicircular canal projection defects. (A-L) Live DIC images of 5dpf wild-type embryos incubated with DMSO, 25μM forskolin or 100μM IBMX between 60 and 90hpf show a gradation in phenotype. A low dose (25μM) of forskolin has little effect on the ear (B,E,H,K). However, treatment with 100μM IBMX can give rise to a severe phenotype, with a swollen ear and unfused projections (C,F,I,L). This is similar to the 'severe' category for the *tb233c* allele, but the swelling is not as extreme as in *tk256a* or *fr24* mutants. The dorsolateral septum (black arrowheads, J-L) and the ventral pillar (asterisks, D-F) have failed to form correctly in the presence of 100μM IBMX. **(M-O)** In situ hybridisation shows an upregulation of the ECM marker *vcana* in unfused canal projections (white arrows, O). Lateral views. Scale bars: A-C, G-I 200μm; D-F, J-L, M-O 50μm. **(P)** Graphical representation of the dataset. Ears swell as a graded response to both forskolin and IBMX concentration. Data were analysed with a 3×3 chi-square contingency table for each drug; $P<0.001$ for both drugs. *N* numbers are shown in parentheses.

Table S1. List of *in situ* hybridisation marker genes, primer sequences and morpholino sequences

Gene	ZFIN ID	Reference
aldh1a3	ZDB-GENE-061128-2	(Pittlik et al., 2008)
atp1a1a.4	ZDB-GENE-001212-4	(Blasiole et al., 2006)
bmp4	ZDB-GENE-980528-2059	(Hammerschmidt et al., 1996)
bmp7b	ZDB-GENE-060929-328	(Shawi and Serluca, 2008)
chsy1	ZDB-GENE-030131-3127	(Thisse and Thisse, 2004)
eya1	ZDB-GENE-990712-18	(Sahly et al., 1999)
fgf8a (fgf8)	ZDB-GENE-990415-72	(Reifers et al., 1998)
foxi1	ZDB-GENE-030505-1	(Solomon et al., 2003)
gpr126	ZDB-GENE-041014-357	This work: the *gpr126* probe used was a 4.6 kb cDNA clone covering the full open reading frame. The cDNA was cloned into the pCRII-TOPO vector, digested with *Not*I and transcribed with SP6.
hapln1a	ZDB-GENE-050302-175	(Kang et al., 2008)
hapln3	ZDB-GENE-040426-2089	(Thisse and Thisse, 2004)
has3	ZDB-GENE-021118-1	(Bakkers et al., 2004)
kcnq1	ZDB-GENE-061214-5	(Abbas and Whitfield, 2009)
mbpa	ZDB-GENE-030128-2	(Brösamle and Halpern, 2002)
pax2a	ZDB-GENE-990415-8	(Pfeffer et al., 1998)
slc12a2 (nkcc1)	ZDB-GENE-040625-53	(Abbas and Whitfield, 2009)
sox9b	ZDB-GENE-001103-2	(Chiang et al., 2001)
tbx1	ZDB-GENE-030805-5	(Piotrowski et al., 2003)
ugdh	ZDB-GENE-011022-1	(Busch-Nentwich et al., 2004)
vcana	ZDB-GENE-011023-1	(Kang et al., 2004)
vcanb	ZDB-GENE-030131-2185	(Kang et al., 2004)

Primer sequences for genotyping

Genomic DNA was amplified using the following primers flanking the mutations: for *tb233c* and *tk256a*, forward 5'-GATGAATCTCAGCACATCACTGC-3' and reverse 5'-GGTCAGTTTGAACTTCATGAGC-3'; for *fr24*, forward 5'-ACTTTGCAAGTACACGTCAGC-3' and reverse 5'-ATTGTCACTGTAAAGCATGCCA-3'.

Morpholino sequences

Gpr126 splice site morpholino: 5'-ATGCTGAAAGACACTCACTCAAAAG-3'

Control 5-base mismatch morpholino: 5'-ATcCTGAAAcACAgTgACTgAAAAG-3'